A particle-tracking model for simulating pollutant dispersion in the Strait of Gibraltar

R. Periáñez *

Departamento Física Aplicada I, E.U. Ingeniería Técnica Agrícola, Universidad de Sevilla, Ctra. Utrera km 1, 41013 Sevilla, Spain

Abstract

A particle-tracking model to simulate the dispersion of contaminants in the Strait of Gibraltar has been developed. The model solves the hydrodynamic equations off-line and tidal analysis is carried out to determine tidal constants for the two main constituents. Tidal constants and residuals are stored in files that are read by the dispersion model. A lagrangian approach is used to solve dispersion; diffusion and decay are simulated by a Monte Carlo method. A method for assessing the areas of the Strait with higher probability of being affected by contamination occurring after an accident in the shipping routes is given. Generally speaking, the fate of a pollutant discharge strongly depends on wind conditions. Winds from the east tend to retain contamination into the Strait. As a consequence, transverse mixing occurs and both Spain and Morocco coasts are affected by contamination. Under calm conditions and west winds, contaminants are flushed out of the Strait faster and transverse mixing does not occur. Thus, only part of Morocco coast has a higher probability of being affected by contamination.

Keywords: Strait of Gibraltar; Tides; Dispersion; Numerical modelling; Pollutant; Particle-tracking

1. Introduction

Numerical models for simulating pollutant dispersion are actually being developed since they can be used for decision-making purposes after releases of contaminants into the marine environment. In particular, particle-tracking methods are well suited for problems in which high contamination gradients are involved, since they do not introduce numerical diffusion. Also, they can give very fast answers, specially if the hydrodynamic calculations are made off-line and tidal analysis and computed residuals are used to reconstruct water movements, which avoids the CFL (Courant–Friederichs–Lewy) limitations in the dispersion calculations. Thus, particle-tracking models are very useful predictive tools that can be used for assessing contamination after accidental or deliberate releases. Particle-tracking models have been used to simulate the dispersion of passive tracers (Harms et al., 2000; Gomez-Gesteira et al., 1999), radionuclides (Schonfeld, 1995; Periáñez and Elliott, 2002), oil spills (Proctor et al., 1994a,b) and even contaminated milk (Elliott et al., 2001) in coastal waters.

Several models have been developed to simulate water circulation and hydrodynamic processes in the Strait of Gibraltar (Izquierdo et al., 2001; Tejedor et al., 1999), but numerical modelling has not been applied to simulate the dispersion of pollutants in the Strait. This is a relevant topic due to the intense shipping activities in the Strait, which include the transport of radioactive material from/to the nuclear fuel reprocessing plants of Sellafield and Cap de la Hague (in UK and France respectively), as well as massive transport of chemical contaminants. Shipping routes are complex, with intersections of longitudinal routes with some several thousands annual transverse rotations Algeciras-Ceuta, Algeciras-Tanger and Tarifa-Tanger (see Fig. 1). Fishing activities in the area must be added. The area of the Strait of Gibraltar has a high ecological and tourist value, and there are also some important towns. A release of contamination into the Strait as a consequence of an accident (or a deliberate release) can lead to relevant ecologic and economic impact.

The objective of this paper consists of describing a particle-tracking dispersion model that could be used for decision-making in the Strait of Gibraltar. The

* Tel.: +34-954486474; fax: +34-954486436.
E-mail address: rperianez@us.es (R. Periáñez).

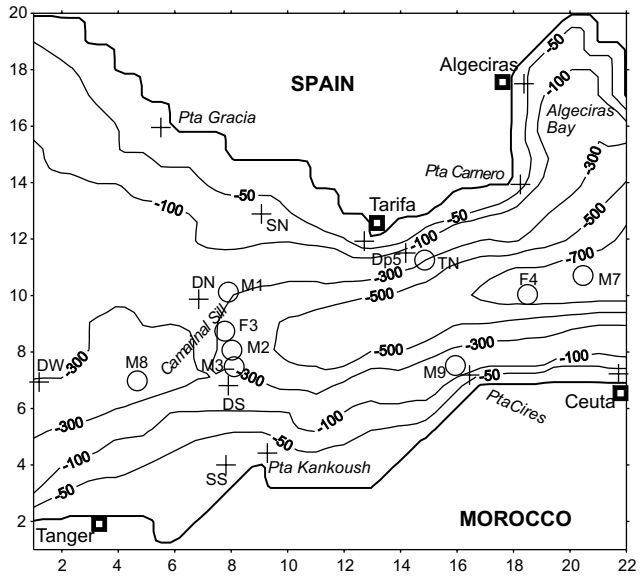

Fig. 1. Map of the computational domain showing some important towns (squares), points where tidal constants were measured (crosses) and where current ellipse parameters were obtained (circles). Each unit in the x and y axis is the grid cell number (thus equal to 2500 m).

hydrodynamic equations are solved off-line, and tidal constants and residual currents are stored in files that will be read by the dispersion code. The model can be applied to simulate the dispersion of a pollutant released at any point in the Strait at any instant of time. Both continuous and instantaneous releases can be simulated. The model provides snap shots of particles at different times during the simulation as well as concentration maps. The areas of the Strait with higher probability of being affected by contamination after hypothetical accidents occurring along shipping routes for several wind conditions have also been found.

Some particulars of the shipping activities and ecologic interest of the area are described in Section 2. The model is presented in the following section. Next, results are presented and discussed in Section 4.

2. The Strait of Gibraltar

The Strait of Gibraltar is the only connection between the Mediterranean Sea and the Atlantic Ocean. As a consequence, there is an intense traffic of merchant vessels: over 70,000 per year, 30% of them declaring hazardous cargos. Also, over 12,000 vessels, mostly passenger ferries, cross the Strait each year between the south and north coasts. Fishing activities must finally be added (Nav42, 1998). Algeciras is the most important port in Spain (and number 25 in the world), with 61.2 Mt of cargo handled in 2003 (Autoridad Portuaria de la Bahía de Algeciras, 2004). Fishing vessels operating from this port are 347, with 6.9 kt catches in 2001.

It is usual to have adverse meteorological conditions in the Strait, with more than 54% of days of moderate to poor visibility and 13% of days with persistent fog conditions (Nav42, 1998). Winds must be added, with frequent east and west gales. East winds (*levantes*) blow an average of 165 days per year, predominantly from April to October, with an average speed of the order of 50 km/h. Maximum speed reaches 125 km/h. Gusts of winds can remain up to 7–10 days. West winds (*ponientes*) blow an average of 60 days per year, from November to March predominantly. Minimum and maximum speeds are 30 and 90 km/h. West winds are not as persistent as *levantes*, lasting for some 12–36 h.

The particular conditions in the area (intense traffic and adverse meteorology) make navigation difficult. Indeed, 81 accidents have occurred in the Strait (Nav42, 1998), with 14 collisions and 16 groundings. For instance, in 1990 there was a collision between the oil tanker Hesperus and the chemical tanker Sea Spirit. More recently, a ferry and a gas tanker collided off Ceuta.

The traffic separation scheme for the Strait is shown in Fig. 2. There is a 0.5 miles wide excluded area whose axis connects the following locations: (35°59.09′ N, 5°25.6′ W)–(35°56.29′ N, 5°36.4′ W)–(35°56.29′ N, 5°44.9′ W). Exterior limits are defined by lines connecting the following points. North limit: (36°1.26′ N, 5°25.6′ W)–(35°58.49′ N, 5°36.4′ W)–(35°58.49′ N, 5°44.9′ W). South limit: (35°52.29′ N, 5°44.9′ W)–(35°53.89′ N, 5°36.4′ W)–(35°56.89′ N, 5°25.6′ W). The north lane is used by ships going from the Mediterranean to the Atlantic. The south lane is used by ships entering the Mediterranean Sea. The coastal navigation zones are defined between the north and south limits of the separation scheme and Spain and Morocco coasts respectively.

The area of the Strait of Gibraltar has a high ecological value, being essential in marine and aerial migratory processes. By decree 57/2003 (4th March, 2003) of the Junta de Andalucía, the Natural Park of Algeciras-Tarifa Coast was created. It consists of 191.3 km^2, 92.47 of which correspond to the marine part of the Park, that extends from Pta Gracia to Pta Carnero (see Fig. 1). A review about geomorphology, flora and fauna of the Park may be consulted in Cabello (2003), but some data are summarized here. Over 1900 species of marine flora and fauna living in the Park have been described. Some of the species with a major interest (due to their endemic character and/or rareness) are sponges like *Axinella estacioi* and jellyfishes (like *Merona ibera*, *Cervera atlantica* and *Scleranthelia microsclera*). There are other 23 species under strict conservation, like *Patella ferruginea* (the largest limpet of European coasts), *Lithophaga lithophaga*, *Pinna nobilis*, *Centrostephanus longispinus*, *Astroides calicularis* etc. As the connection between the Mediterranean Sea and the Atlantic Ocean,

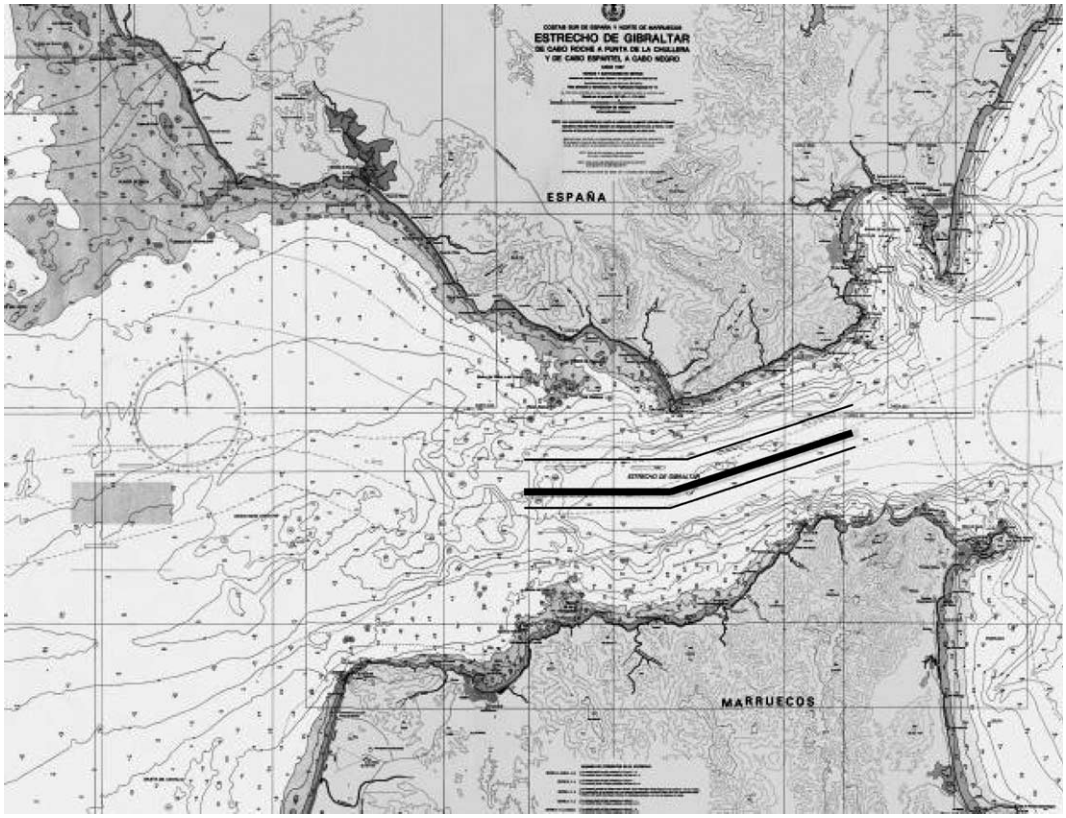

Fig. 2. Traffic separation scheme in the Strait of Gibraltar.

marine turtles and mammals (dolphin, porpoise, sperm whale, killer whale) travel through the Strait. Finally, the 15 km of fine sand beaches in the Park and other cultural resources (archeological Roman ruins of Baelo Claudia and some 30 caves with palaeolithic art) have a high tourist interest.

3. The model

A 2D barotropic model is used. An important feature of the tidal flow in the Strait is that it can be considered, as a first approach, as barotropic. Indeed, 93% of the variance of current velocity in the semidiurnal band has a barotropic character in the Strait (Mañanes et al., 1998). Tsimplis and Bryden (2000) have pointed out that tidal currents are barotropic and larger than the mean inflow or outflow. The semidiurnal tide dominates ADCP (Acoustic Doppler Current Profiler) records in the Strait, obscuring the expected two-layer character of the mean flow. The tidal signal is so strong that it reverses the currents near the bottom for a part of each tidal cycle. As a consequence, 2D depth-averaged models have already been applied to simulate surface tides in the Strait (see for instance Sánchez and Pascual, 1988; Tejedor et al., 1999). Tsimplis et al. (1995) have even used a 2D barotropic model for simulating tides in the whole Mediterranean Sea. The success of these models indicates that the baroclinic component is of secondary importance. However, it is also known that the surface manifestation of baroclinic tidal currents is usually small. Nevertheless, pollutants considered in this work are released at (or near to) the sea surface and remain close to the surface after the typical simulated times (several days), as discussed in Section 4. Thus, the use of a 2D depth-averaged barotropic model to obtain surface currents is justified.

The depth-averaged hydrodynamic equations may be written as:

$$\frac{\partial z}{\partial t}+\frac{\partial}{\partial x}(Hu)+\frac{\partial}{\partial y}(Hv)=0 \tag{1}$$

$$\frac{\partial u}{\partial t}+u\frac{\partial u}{\partial x}+v\frac{\partial u}{\partial y}+g\frac{\partial z}{\partial x}-\Omega v+\frac{\tau_u}{\rho H}=A\left(\frac{\partial^2 u}{\partial x^2}+\frac{\partial^2 u}{\partial y^2}\right) \tag{2}$$

$$\frac{\partial v}{\partial t}+u\frac{\partial v}{\partial x}+v\frac{\partial v}{\partial y}+g\frac{\partial z}{\partial y}+\Omega u+\frac{\tau_v}{\rho H}=A\left(\frac{\partial^2 v}{\partial x^2}+\frac{\partial^2 v}{\partial y^2}\right) \tag{3}$$

where u and v are the depth-averaged water velocities along the x and y axis, D is the depth of water below the mean sea level, z is the displacement of the water surface above the mean sea level measured upwards, $H = D + z$ is the total water depth, Ω is the Coriolis parameter ($\Omega = 2w \sin \beta$, where w is the earth rotational angular velocity and β is latitude), g is acceleration due to gravity, ρ is water density and A is the horizontal eddy viscosity. τ_u and τ_v are friction stresses that have been written in terms of a quadratic law:

$$\begin{aligned} \tau_u &= k\rho u\sqrt{u^2 + v^2} \\ \tau_v &= k\rho v\sqrt{u^2 + v^2} \end{aligned} \tag{4}$$

where k is the bed friction coefficient.

The solution of these equations provides the water currents at each point in the model domain and for each time step. Currents are treated through standard tidal analysis and tidal constants are stored in files that will be read by the dispersion code to calculate the advective transport of particles. The model includes the two main tidal constituents, M_2 and S_2. Thus, the hydrodynamic equations are solved for each constituent and tidal analysis is also carried out for each constituent separately. A residual transport cannot be produced by the pure harmonic currents given by the tidal analysis, thus residuals have also been calculated for each constituent.

Some open boundary conditions must be provided to solve the hydrodynamic equations. Surface elevations are specified, from observations, along open boundaries of the computational domain. A radiation condition is applied to the water velocity component that is normal to the open boundary:

$$\frac{\partial \phi}{\partial t} = c\frac{\partial \phi}{\partial n} \tag{5}$$

where ϕ is the current component normal to the boundary, in the direction n, and c is a phase speed calculated as in Jensen (1998). Water flux across a land boundary is set to zero as usual.

The model uses a particle-tracking approach to simulate advection and diffusion of pollutants. Advection is computed solving the following equation for each particle:

$$\frac{\mathrm{d}\mathbf{r}}{\mathrm{d}t} = \mathbf{q} \tag{6}$$

where $\mathbf{r}$ is the position vector of the particle and $\mathbf{q}$ is the current vector solved in components u and v.

The particle-tracking model is three-dimensional, but the hydrodynamic calculations provide depth-averaged currents. In the main body of water above the logarithmic layer, the flow gradually increases in a manner which may be represented as (Pugh, 1987):

$$u_{z'} = u_s\left(\frac{D - z'}{D}\right)^{1/m} \tag{7}$$

where $u_{z'}$ is the current speed at a level z' below the sea surface and u_s is the surface flow. From observations, it has been deduced that m ranges between 5 and 7. The surface current can be deduced from the depth-averaged one (Pugh, 1987):

$$u_s = \frac{m+1}{m}\bar{u} \tag{8}$$

where $\bar{u}$ is the depth-averaged current. Thus, components u and v of the current at any depth can be obtained from their depth-averaged values (provided by the hydrodynamic model) applying Eqs. (7) and (8). This current profile has also been used by Riddle (1998) in a particle-tracking model.

Wind is typically included in particle-tracking models assuming that the surface wind-induced current is 3% of the wind speed measured 10 m above the sea surface (Pugh, 1987; Proctor et al., 1994a). This current decreases logarithmically to zero at a depth z_1, that is assumed to be 20 m (Elliott, 1986). The wind-induced current at any depth may thus be written as (Pugh, 1987):

$$u_{z'} = \begin{cases} u_0 - \frac{u^*}{\kappa}\ln\left(\frac{z'}{z_0}\right) & \text{if } z' < z_1 \\ 0 & \text{if } z' \geqslant z_1 \end{cases} \tag{9}$$

where u_0 is the surface wind-induced current, $\kappa = 0.4$ is the von Karman constant, u^* is a friction velocity and z_0 is the sea surface roughness length, which has values between 0.5 and 1.5 mm. It has been obtained (Pugh, 1987) that the friction velocity can be estimated as

$$u^* = 0.0012W \tag{10}$$

for a wide range of conditions, where W is wind speed 10 m above the sea surface. From these equations, the wind effect on the advection of particles can be calculated. Of course, the current profile is solved in the u and v components.

Three-dimensional diffusion is simulated using a random walk method (Proctor et al., 1994a; Hunter, 1987; Periáñez and Elliott, 2002). It has been shown that it is a simulator of Fickian diffusion provided that the maximum sizes of the horizontal and vertical steps, D_h and D_v respectively, are:

$$\begin{aligned} D_h &= \sqrt{12K_h\Delta t} \\ D_v &= \sqrt{2K_v\Delta t} \end{aligned} \tag{11}$$

where K_h and K_v are the horizontal and vertical diffusion coefficients respectively.

Decay of particles is also included (this is relevant for instance in the case of radioactive discharges) as usually in particle-tracking models (Hunter, 1987; Proctor et al., 1994a; Periáñez and Elliott, 2002). It must be clearly pointed out that in its present form, the model is valid for dissolved chemical pollutants in general (decay would generally be zero), being radioactive elements a

particular case in which decay is described by the radioactive decay constant.

Other processes are relevant in the case of oil spills, as evaporation from the surface and biodegradation. These processes are also described by means of a decay constant (see for instance Proctor et al., 1994a). Buoyancy is described by an upwards advection velocity that depends on the size of droplets, oil and water densities and water viscosity. The effects of surface tension and oil weathering are generally not included in oil spill models (Proctor et al., 1994a; Elliott, 1999). Thus, the inclusion of the rise velocity caused by the buoyant force would be the only modification required to simulate oil spills with this model.

Both instantaneous and continuous releases can be simulated. From the total amount of pollutant discharged, concentration maps can be obtained by counting the density of particles per water volume unit. Date and time of the discharge (and duration in the case of continuous releases) must be specified since the fate of the release will depend on the tidal state when it took place. Thus, the appropriate phase of each tidal constituent at $t = 0$ must be specified. The values used in this model correspond to the origin of time being January 1, 2003 at 0:15 h Greenwich time.

The adsorption of pollutants by suspended and bottom sediments can also be simulated with a particle-tracking model (Periáñez and Elliott, 2002). However, these processes are neglected in the present study since suspended matter concentrations are very low in the Strait, typically 0.1–0.5 mg/L (León-Vintró et al., 1999). Also, average depth is 350 m (reaching 900 m in the eastern part) and, as a consequence, interactions of pollutants with bed sediments can also be neglected.

The hydrodynamic equations are solved using a explicit finite difference scheme on a grid with resolution $\Delta x = \Delta y = 2500$ m. Time step, limited by the CFL condition is $\Delta t = 5$ s. Once a stable periodic solution is achieved, tidal analysis is carried out to determine tidal constants that are used by the particle-tracking code. Residual transports are also calculated. This is done for the M_2 and S_2 tides separately. While there is no stability criterion equivalent to the CFL condition in the particle-tracking calculations, it is wise to ensure that each particle does not move through a distance that exceeds the grid spacing during each time step. This was satisfied by using a time step of 600 s.

4. Results and discussion

After a calibration process, the bed friction coefficient was fixed as $k = 0.050$. The horizontal eddy viscosity is $A = 10$ m^2/s. In general, good agreement between model results and observations are obtained with these values.

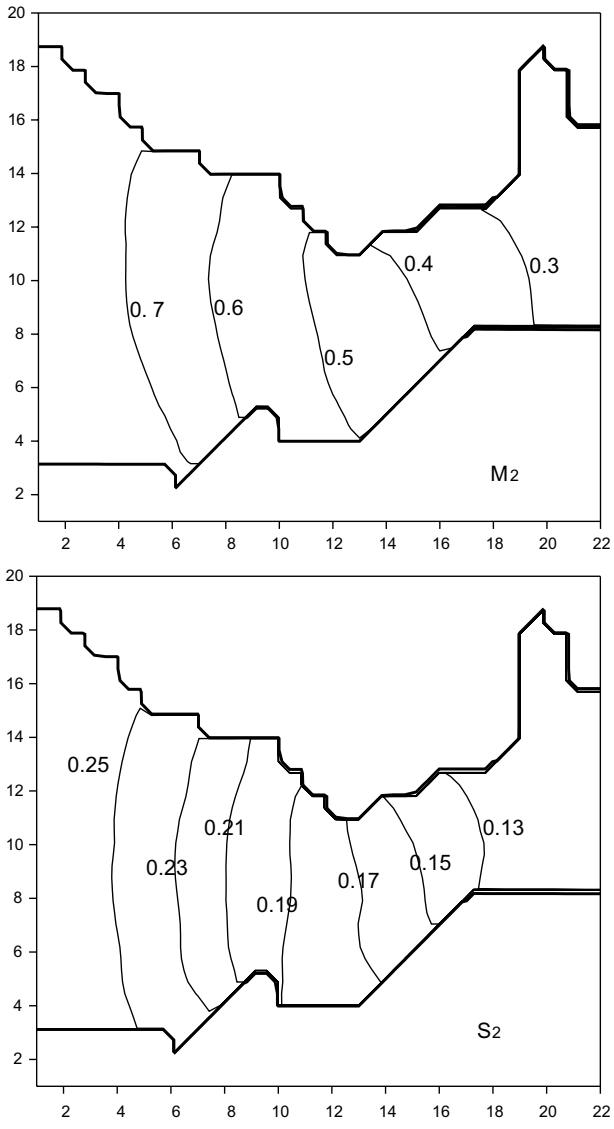

Fig. 3. Computed corange charts for the M_2 and S_2 tides. Amplitudes are given in m.

Computed corange maps for the M_2 and S_2 tide are presented in Fig. 3. They are similar to those obtained from observations (Candela et al., 1990) and to the computed by Tejedor et al. (1999). They show an amplitude reduction in a factor 2 approximately along the Strait in both tides, and essentially constant amplitudes across the Strait. Good quantitative agreement is also obtained. Observed and computed amplitudes and phases of both tides at several locations in the Strait, shown in Fig. 1, are given in Table 1. In the case of the M_2 tide, the maximum difference between observed and computed amplitudes is 7.8 cm, being the average of the absolute values of the deviations 4 ± 2 cm. For phases, maximum difference between observations and computations is 10°, with an average of the absolute values of the deviations equal to 4 ± 4°. In the case of the S_2 tide,

Table 1
Observed and computed amplitudes (cm) and phases (deg) of tidal elevations

Station	M_2				S_2			
	A_{obs}	g_{obs}	A_{comp}	g_{comp}	A_{obs}	g_{obs}	A_{comp}	g_{comp}
Pta Gracia	64.9	49	70.5	57	22.3	74	24.8	81
DN	60.1	52	60.9	57	22.5	74	22.0	82
DS	54.0	62	59.1	61	21.1	83	20.9	86
SN	52.3	48	55.9	53	18.5	73	20.6	78
SS	57.1	67	64.9	66	20.6	92	22.5	91
DW	78.5	56	78.5	64	29.0	82	27.0	89
Pta Kankoush	51.8	69	52.7	59	20.1	90	18.9	86
Tarifa	41.5	57	46.2	52	14.2	85	17.4	77
Dp5	44.4	48	42.8	51	16.1	74	16.3	76
Pta Cires	36.4	47	38.5	56	14.1	74	14.3	82
Algeciras	31.0	48	25.0	48	11.1	74	10.0	71
Pta Carnero	31.1	48	25.6	46	11.5	71	10.4	69
Ceuta	29.7	50	25.0	50	11.4	76	10.0	72

Table 2
Observed and computed amplitudes (q, m/s) and phases (g, deg) of the M_2 and S_2 barotropic tidal velocities at several locations

Station	M_2				S_2			
	q_{obs}	g_{obs}	q_{comp}	g_{comp}	q_{obs}	g_{obs}	q_{comp}	g_{comp}
M3	0.91	147	0.96	139	0.31	171	0.32	180
M7	0.25	160	0.44	145	0.12	178	0.16	176
M8	0.65	157	0.57	148	0.23	182	0.20	178

Table 3
Comparison of several current ellipse parameters between this model and the model of Tejedor et al. (1999)

Station	M_2				S_2			
	M	dir	m	g	M	dir	m	g
Tejedor et al. (1999)								
M1	0.96	351	0.07	158	0.29	351	0.02	181
M2	1.08	7	0.07	164	0.33	7	0.04	189
M3	1.12	9	0.06	162	0.34	9	0.03	189
M7	0.40	25	0.13	155	0.12	20	0.03	181
M8	0.63	15	0.007	160	0.19	13	0.008	188
M9	0.71	26	0.03	169	0.21	24	0.001	191
F3	1.07	6	0.08	164	0.33	7	0.04	189
F4	0.45	16	0.04	161	0.14	16	0.007	184
TN	0.68	25	0.07	157	0.20	22	0.008	182
This model								
M1	0.95	353	0.008	160	0.36	352	0.04	171
M2	1.14	3	0.06	140	0.40	4	0.05	180
M3	0.96	1	0.06	139	0.32	3	0.03	180
M7	0.44	4	0.11	145	0.16	6	0.05	176
M8	0.57	10	0.05	148	0.20	9	0.01	178
M9	0.67	20	0.008	166	0.24	21	0.003	175
F3	1.02	1	0.01	132	0.36	359	0.04	178
F4	0.52	8	0.06	147	0.18	9	0.02	178
TN	0.66	12	0.02	128	0.30	13	0.02	171

M (m/s): major axis magnitude, dir (deg): orientation of the axis anticlockwise from east, m (m/s): minor axis magnitude, g (deg): phase of the current.

maximum deviation in amplitudes is 3.2 cm, with an average of their absolute values equal to 1.4 ± 1.0 cm. The corresponding maximum and average values for phases are 8.6° and 4.7 ± 2.5°.

A comparison between computed and barotropic current amplitudes and phases deduced from measurements in the Strait can be seen in Table 2. The agreement in current amplitudes is not so good as in the case

of tidal elevations, specially for the M_2 tide. However, the difficulty in appropriately defining the barotropic current has already been commented by Tejedor et al. (1999) when they compared barotropic currents predicted by their model with those derived from observations in the Strait. Nevertheless, as can be observed in Table 3, the agreement between several ellipse parameters calculated by both models is generally good. Thus, it seems that the present model gives a representation of the Strait that is realistic enough to implement on it the particle-tracking dispersion code.

Values for the diffusion coefficients have to be provided. The horizontal diffusion coefficient depends on the horizontal grid spacing. Following Dick and Schonfeld (1996):

$$K_h = 0.2055 \times 10^{-3} \Delta x^{1.15} \quad (12)$$

The present grid resolution gives $K_h = 1.7$ m^2/s. For the vertical diffusion coefficient a typical value of 0.001 m^2/s is used (Elliott et al., 2001; Schonfeld, 1995; Dick and Schonfeld, 1996; Elliott, 1999).

An example of the type of results that can be obtained from the particle-tracking model is presented in Fig. 4. Decay of particles is not considered in all simulations described in this paper. An instantaneous discharge of a pollutant is carried out into grid cell (7,9), in the area of Camarinal Sill, during high water at Tarifa and with no wind. Three thousand particles are used in the simulation, whose tracks are followed during two days. The position of each particle at four different times after the release is shown in Fig. 4 (top). The concentration of the pollutant in arbitrary units per m^3 at $t = 48$ h is also presented in Fig. 4 (center). There is a net transport towards the Mediterranean Sea, although the patch moves forward and backward following tidal oscillations. This can be also seen in Fig. 4 (down), where the time evolution of the number of particles inside an arbitrary grid cell [in this case (15,9)] is shown. The patch moves three times over this point, producing three peaks in the number of particles at 21, 26 and 36 h after the release. The highest peak, 254 particles, is observed 26 h after the release. In this simulation 1.0×10^6 units of contaminant where released, thus the peak implies a maximum concentration equal to 9.2×10^{-5} units/m^3. For the following peak, at $t = 36$ h, the concentration is reduced in a factor 5 due to the spreading of the patch. From the position of the center of the patch after 48 h, it can be estimated an average velocity of the pollutant (at the surface) equal to 17 cm/s directed towards the Mediterranean. This number can be compared with the mean speed of the Atlantic inflow, of some 23 cm/s above 90 m, measured by Tsimplis and Bryden (2000).

Generally speaking, a contamination patch released in the central region of the Strait will be flushed out the model domain after a few days (depending on wind conditions). However, these initial days are the most

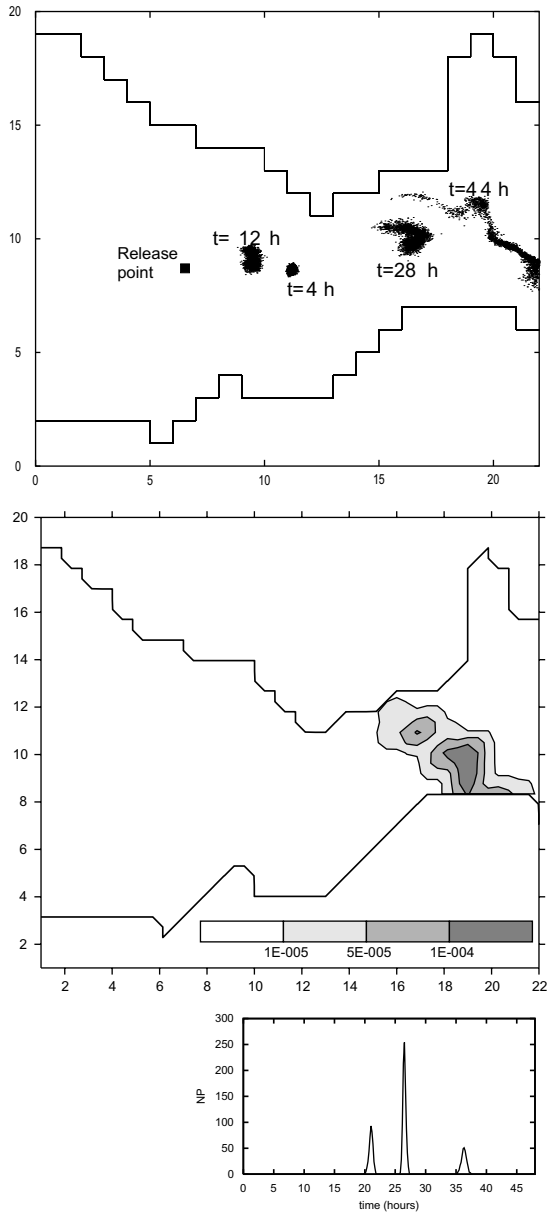

Fig. 4. Up: Dispersion of an instantaneous release. The position of particles at different times after the release is shown. Center: Computed surface concentration in arbitrary units per m^3 48 h after the release (obtained from the density of particles). Down: Time evolution of the number of particles inside grid cell (15,9).

relevant from a decision-making point of view, since pollutant concentrations are higher and, as a consequence, risk (for instance dose in the case of a radioactive release) is also higher. Nevertheless, if the accident occurs close to the shoreline, the time required to flush out contaminants increases. Two accidents (instantaneous releases during high water at Tarifa and under calm conditions) have been simulated close to both shores of the Strait. The positions of particles 7 days (accident in the north) and 5 days (accident in the south) after the release are shown in Fig. 5. In these

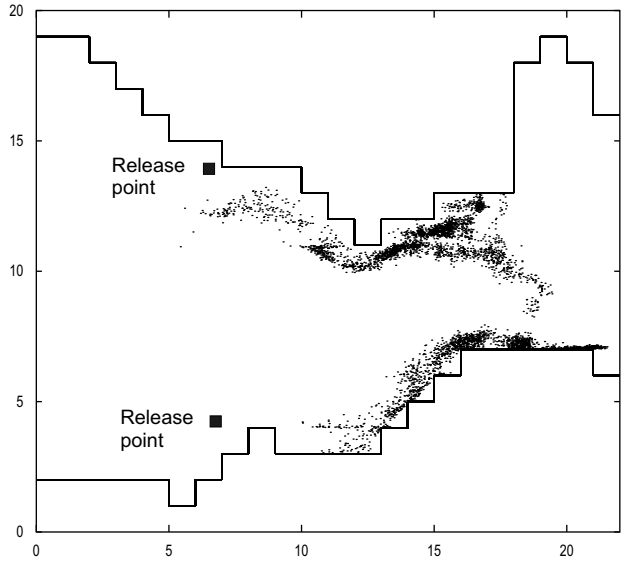

Fig. 5. Position of particles 7 days (accident in the north) and 5 days (accident in the south) after the releases occurring in the points indicated in the map.

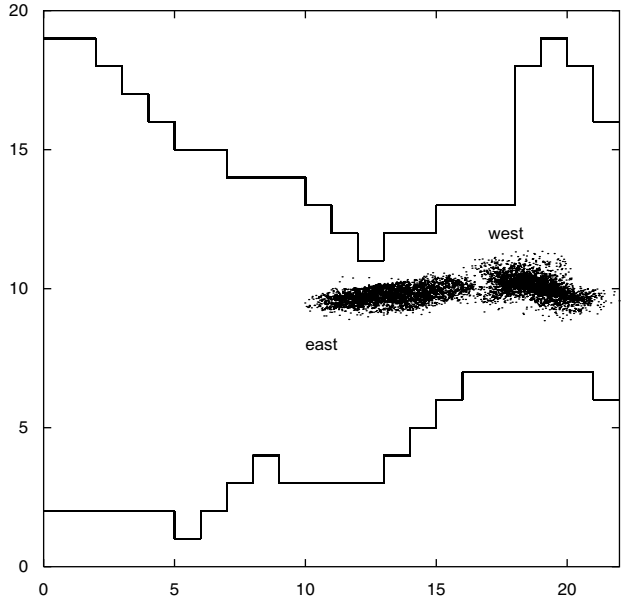

Fig. 6. Position of particles 28 h after an instantaneous release at grid cell (7,9) with 15 m/s winds from the east and west.

cases contamination moves along the coast, oscillating in the east–west direction with tides, during a longer period of time. It is due to the fact that currents are weaker along the shores than in the central part of the Strait.

It has been obtained that after a simulation over 7 days, the maximum depth reached by particles is of some 50 m. Thus, as was commented in Section 3, contaminants released at the surface remain in the top of the water column.

The movement of a patch is obviously influenced by wind conditions. This can be clearly seen with the help of Fig. 6. The same simulation presented in Fig. 4 has been repeated but with 15 m/s east and west winds. The position of particles 28 h after the release for both simulations is shown in Fig. 6, that can be compared with the 28 h patch in Fig. 4. West winds, directed in the same direction as the residual circulation, produce a faster movement to the eastern part of the Strait, while east winds tend to retain particles into the Strait. Since the particle-tracking model is three-dimensional, shear diffusion is produced and the patch size increases in the direction of wind.

An example of the simulation of a continuous release is presented in Fig. 7. The release occurs at same point and tidal conditions as before (cell (7,9) and high water at Tarifa), and under calm wind. The position of particles 44 h after the release is shown in Fig. 7. This can be compared with the 44 h patch in Fig. 4. Now there is a plume extending from the release point to the eastern part of the Strait. It is interesting to observe that four patches with higher concentrations of particles are apparent in the plume. They correspond to particles released during slack water, that remain concentrated and move together.

We are interested on finding the areas of the Strait that have higher probability of being affected by contamination after an accident. To do this, the integral $I_{i,j}$ is defined as:

$$I_{i,j} = \int_0^T C_{i,j}\,\mathrm{d}t \tag{13}$$

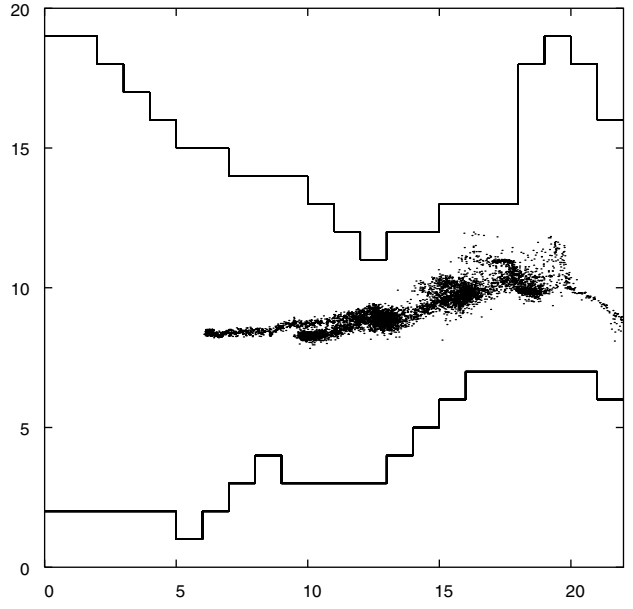

Fig. 7. Position of particles 44 h after the beginning of a continuous release at grid coordinates (7,9).

where $C_{i,j}$ is pollutant concentration at point i, j and T is the simulation time. Thus, $I_{i,j}$ gives the area under the curve that represents the time evolution of pollutant concentration at point i, j. This quantity is calculated for each point in the model domain and all $I_{i,j}$ are normalized to its maximum value. Thus, the magnitude $P_{i,j}$ is obtained as:

$$P_{i,j} = \frac{I_{i,j}}{\max(I_{i,j})} \tag{14}$$

$P_{i,j}$, that ranges between 0 and 1, is mapped over the model domain and the map is used to define the areas of the Strait with a higher probability of being affected by contamination after an accident. It must be pointed out that P does not give any absolute probability of contamination, but it can merely be used to compare different points in the Strait. The areas with lower P values will have a higher probability of remaining unaffected than the areas of higher P values. A limitation of this approach is that points in which there is an intense peak with short temporal duration cannot be distinguished from points in which lower concentrations are obtained over longer times. Also, P does not give information about the magnitude of the peak, although this information can be obtained from the model (see Fig. 4). The spread of a contaminant patch depends on the tidal state when the release occurs and on wind conditions. Thus, four accidents have been simulated for each point located along traffic lanes shown in Fig. 2. These four accidents are considered to occur at high water, ebb, low water and flood. The values of $P_{i,j}$ for each of the four accidents occurring for several points along traffic lanes have been averaged and represented in Fig. 8. Three points along lanes have been used to simulate the four accidents. They correspond to the west, central and east Strait and have grid coordinates (5,8), (13,8) and (18,10). Three different wind conditions have also been considered: calm wind, east and west winds (which are dominant in the Strait). Thus, each map represents the average of $P_{i,j}$ over 12 values. The duration T of each simulation is long enough to allow particles to be flushed off the Strait, and ranges from 1 to 7 days.

Results in Fig. 8 indicate that the area that is more affected by contamination is the central part of the Strait (shipping route). This is an obvious result, but it is interesting to note that, in general, the coast of Africa (from Pta Cires to the town of Ceuta) is more exposed to contamination than the Spanish coast. The strong west–east currents in the Strait inhibits mixing in the transverse direction, thus the coast remains relatively clean. In the case of winds blowing from the east, the wind-induced current is in the opposite direction than the residual current. Thus, contaminants are retained into the Strait for a longer time, allowing transverse mixing to occur. As a consequence, the Spanish coast is also affected, specially from Tarifa to Pta Carnero. West

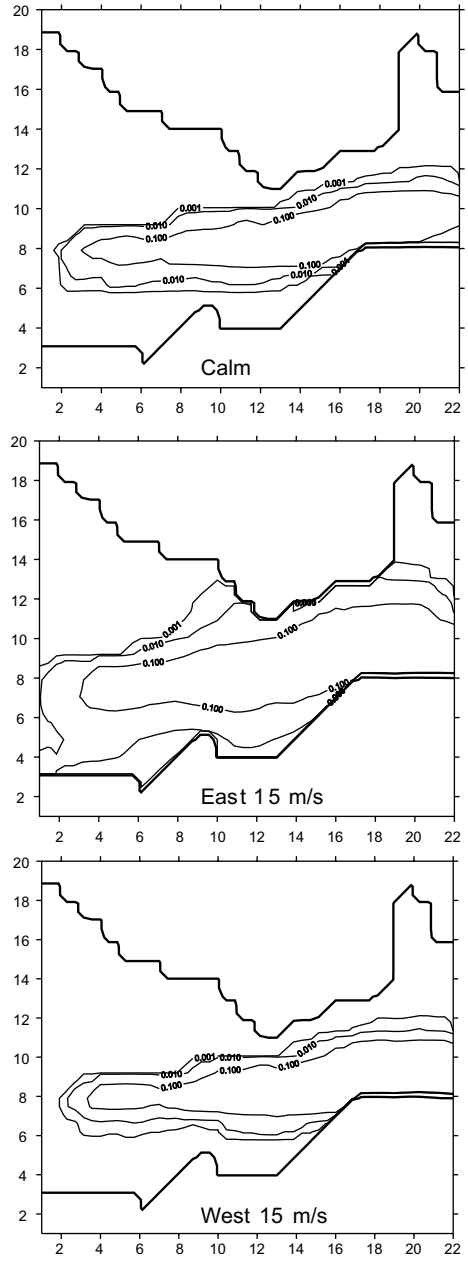

Fig. 8. Values of P for three different wind conditions averaged for accidents occurring at three points along traffic lanes and four tidal states for each point. Thus, each map represents an average over 12 P values for each point in the domain.

winds are in the same direction as the residual current and, as a consequence, produce a faster flushing of particles, but the map is essentially the same as that obtained for calm conditions.

Finally, an accident has been simulated at Algeciras harbor. The accident consisted of an instantaneous release occurring during high water at Tarifa. It has been found that contaminants are retained into Algeciras Bay. Only in the case of winds blowing from the north contaminants would be flushed out the Bay. The position of particles for calm conditions and a 15 m/s

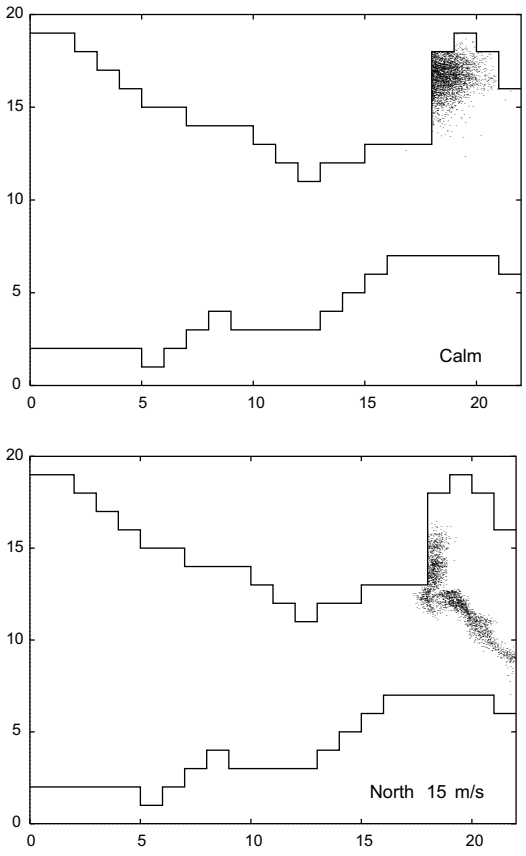

Fig. 9. Position of particles after an accident at Algeciras harbor, 14 days after the accident in the case of calm conditions and 2 days after the accident in the case of a 15 m/s north wind.

northern wind, 14 and 2 days after the release respectively, is presented in Fig. 9. It can be seen that for calm wind essentially all the contamination is retained into the Bay (this would also be the case for east and west winds). In the case of north winds, contaminants are transported to the axis of the Strait. From this area they are flushed out by longitudinal currents. In the case of a radioactive or toxic chemical spill, impact on population will be higher if the contaminant is retained into the Bay since concentrations remain higher (also during a longer time) and the contamination source is closer to Algeciras as well. This accident would represent the highest risk on local population.

5. Conclusions

A particle-tracking model for simulating pollutant dispersion in the Strait of Gibraltar has been developed. The model solves the depth-averaged hydrodynamic equations for the M_2 and S_2 tidal constituents off-line. Tidal analysis is carried out and tidal constants and residuals are stored in files that are read by the dispersion model. Dispersion is solved using a lagrangian approach, diffusion and decay being simulated by means of a Monte Carlo method. The dispersion model is three-dimensional, thus standard vertical profiles for the tidal and wind-induced currents have been used to define the variation of currents with depth.

Computed tide amplitudes and current ellipse parameters for both constituents are, in general, in good agreement with observations in the Strait and with earlier computations. Thus, it seems that the hydrodynamic description is realistic enough to implement pollutant dispersion on it. Some examples on the dispersion of contaminants have been provided. Generally speaking, the fate of a patch depends on the tidal state when the release was carried out and on wind conditions. A method to assess the areas of the Strait that may be more affected by contamination after an accident occurring in the shipping routes has been provided. Winds from the east, as opposite to the residual current, tend to retain contaminants in the Strait. This enhances mixing in the transverse direction and contaminants may reach both the African and Spanish coasts. Under calm conditions and winds from the west a faster cleaning of the Strait takes place. Transverse mixing does not occur and only part of the north-African coast has a higher probability of being affected by contamination.

The accident that implies the highest risk on local population would take place at, or near, Algeciras harbor. In this case contamination stays into Algeciras Bay. A faster flushing of contaminants out of the Bay occurs only if wind blows from the north sector.

Acknowledgements

The author is indebted to Mr. A. Serrano, from Centro Zonal de Coordinación de Salvamento de Tarifa, for kindly providing information on the traffic separation scheme in the Strait.

References

Autoridad Portuaria de la Bahía de Algeciras, 2004. Web site http://www.apba.es (in English and Spanish).

Cabello, J., 2003. Parque Natural del Estrecho, un nuevo futuro. Revista Medio Ambiente 43. Available from <http://www.juntadeandalucia.es/medioambiente> (in Spanish).

Candela, J., Winant, C., Ruiz, A., 1990. Tides in the Strait of Gibraltar. Journal of Geophysical Research 95, 7313–7335.

Dick, S., Schonfeld, W., 1996. Water transport and mixing in the North Frisian Wadden Sea. Results of numerical investigations. German Journal of Hydrography 48, 27–48.

Elliott, A.J., 1986. Shear diffusion and the spread of oil in the surface layers of the North Sea. German Journal of Hydrography 39, 113–137.

Elliott, A.J., 1999. Simulations of atmospheric dispersion following a spillage of petroleum at sea. Spill Science and Technology Bulletin 5, 39–50.

Elliott, A.J., Wilkins, B.T., Mansfield, P., 2001. On the disposal of contaminated milk in coastal waters. Marine Pollution Bulletin 42, 927–934.

Gomez-Gesteira, M., Montero, P., Prego, R., Taboada, J.J., Leitao, P., Ruiz-Villareal, M., Neves, R., Perez-Villar, V., 1999. A two-dimensional particle-tracking model for pollution dispersion in A Coruña and Vigo Rias (NW Spain). Oceanologica Acta 22, 167–177.

Harms, I.H., Karcher, M.J., Dethleff, D., 2000. Modelling Siberian river runoff—implications for contaminant transport in the Artic Ocean. Journal of Marine Systems 27, 95–115.

Hunter, J.R., 1987. The application of lagrangian particle tracking techniques to modelling of dispersion in the sea. In: Noye, J. (Ed.), Numerical Modelling. Applications to Marine Systems. Elsevier/North-Holland, pp. 257–269.

Izquierdo, A., Tejedor, L., Sein, D.V., Backhaus, J.O., Brandt, P., Rubino, A., Kagan, B.A., 2001. Control variability and internal bore evolution in the Strait of Gibraltar: a 2D two-layer model study. Estuarine Coastal and Shelf Science 53, 637–651.

Jensen, T.G., 1998. Open boundary conditions in stratified ocean models. Journal of Marine Systems 16, 297–322.

León-Vintró, L., Mitchell, P.I., Condren, O.M., Downes, A.B., Papucci, C., Delfanti, R., 1999. Vertical and horizontal fluxes of plutonium and americium in the western Mediterranean and the Strait of Gibraltar. The Science of the Total Environment 237, 77–91.

Mañanes, R., Bruno, M., Alonso, J., Fraguela, B., Tejedor, L., 1998. Non-linear interaction between tidal and subinertial barotropic flows in the Strait of Gibraltar. Oceanologica Acta 21, 33–46.

Nav42, 1998. Report to the Maritime Safety Committee. International Maritime Organization. Available from <http://www.navcen.uscg.gov/marcomms/imo/document.htm>.

Periáñez, R., Elliott, A.J., 2002. A particle tracking method for simulating the dispersion of non-conservative radionuclides in coastal waters. Journal of Environmental Radioactivity 58, 13–33.

Proctor, R., Flather, R.A., Elliott, A.J., 1994a. Modelling tides and surface drift in the Arabian Gulf: application to the Gulf oil spill. Continental Shelf Research 14, 531–545.

Proctor, R., Elliott, A.J., Flather, R.A., 1994b. Forecast and hindcast simulations of the Braer oil spill. Marine Pollution Bulletin 28, 219–229.

Pugh, D.T., 1987. Tides, Surges and Mean Sea Level. Wiley, Chichester.

Riddle, A.M., 1998. The specification of mixing in random walk models for dispersion in the sea. Continental Shelf Research 18, 441–456.

Sánchez, P., Pascual, J.R., 1988. Primeras experiencias en la modelización del Estrecho de Gibraltar. In: Almazán, J.L. (Ed.), Oceanografía Física del Estrecho de Gibraltar. Escuela Superior de Ingenieros de Caminos, Madrid, pp. 251–282 (in Spanish).

Schonfeld, W., 1995. Numerical simulation of the dispersion of artificial radionuclides in the English Channel and the North Sea. Journal of Marine Systems 6, 529–544.

Tejedor, L., Izquierdo, A., Kagan, B.A., Sein, D.V., 1999. Simulation of the semidiurnal tides in the Strait of Gibraltar. Journal of Geophysical Research 104, 13541–13557.

Tsimplis, M.N., Bryden, H.L., 2000. Estimations of the transports through the Strait of Gibraltar. Deep Sea Research 47, 2219–2242.

Tsimplis, M.N., Proctor, R., Flather, R.A., 1995. A two dimensional tidal model for the Mediterranean Sea. Journal of Geophysical Research 100, 16223–16239.